

## Proteomic Analysis of Human Transplanted Submandibular Gland in Patients with Epiphora after Transplantation

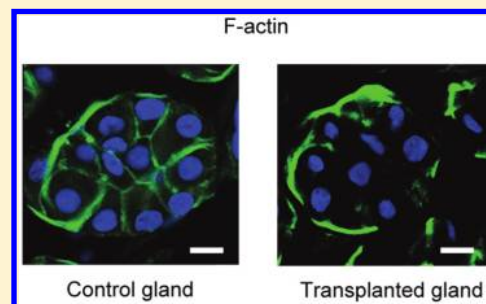
Chong Ding,<sup>†</sup> Yan Zhang,<sup>†</sup> Xin Peng,<sup>‡</sup> Yang Wang,<sup>‡</sup> Lei Zhang,<sup>‡</sup> Xin Cong,<sup>†</sup> Qian-Wen Ding,<sup>‡</sup> Ruo-Lan Xiang,<sup>†</sup> Li-Ling Wu,<sup>\*,†</sup> and Guang-Yan Yu<sup>\*,‡</sup>

<sup>†</sup>Center for Salivary Gland Diseases of Peking University School and Hospital of Stomatology, Department of Physiology and Pathophysiology, Peking University Health Science Centre and Key Laboratory of Molecular Cardiovascular Sciences, Ministry of Education, Beijing, China

<sup>‡</sup>Department of Oral and Maxillofacial Surgery, Peking University School and Hospital of Stomatology, Beijing, China

**ABSTRACT:** Submandibular gland autotransplantation is effective for treating severe dry eye syndrome. However, more than 40% of patients show epiphora within 3–6 months after treatment. The mechanism underlying the hypersecretion in epiphora remains to be elucidated for developing novel interventions. Since salivary gland secretion is dependent on a variety of proteins, we analyzed the changes in protein expression in transplanted glands of epiphora patients with 2-D gel electrophoresis and electrospray ionization quadrupole/time-of-flight mass spectrometry and evaluated their possible roles in epiphora. There were 23 proteins that showed altered expression in the glands of epiphora patients, 15 being up-expressed and 8 being down-expressed. The expression of secretory proteins was decreased in these glands, including alpha-amylase, cystatin S, SA, and SN. In contrast, cytoskeletal proteins were all up-regulated, including actin and vimentin. Immunofluorescence revealed that the intensity ratio of F-actin in apical and lateral cytoplasm to total F-actin in acini was decreased in the glands of epiphora patients. Carbachol stimulation induced a similar redistribution of F-actin in the control glands. Phosphorylation of extracellular signal-regulated kinase 1/2 (ERK1/2) was increased in both carbachol-stimulated and epiphora glands. Preincubation of submandibular glands with ERK1/2 inhibitors PD98059 or U0126 inhibited carbachol-induced F-actin redistribution. These results indicated that differentially expressed proteins participated in the hypersecretion of transplanted submandibular glands and the redistribution of F-actin might be involved in this hypersecretion in an ERK1/2-dependent manner.

**KEYWORDS:** submandibular gland, transplantation, epiphora, proteome, filamentous actin, extracellular signal-regulated kinase 1/2, hypersecretion



### INTRODUCTION

Dry eye syndrome is a relatively common ophthalmological disorder characterized by reduced or lack of tears and has serious complications. Despite the generally efficient pharmaceutical tear substitutes or the occlusion of the lacrimal drainage pathways for patients with mild or moderate dry eye syndrome, severely affected patients do not achieve adequate relief and corneal changes, even loss of vision, often occur.<sup>1</sup>

Transplantation of an autologous submandibular gland into the temporal fossa with insertion of Wharton's duct into the upper conjunctival fornix was first reported as treatment for severe dry eye syndrome in 1986.<sup>2</sup> Since then, several reports revealed the stable function of the transplanted gland for at least 5–10 years after surgery, which provided a continuous, endogenous source of ocular lubrication that could substantially improve clinical manifestations and reduce the cornea damage.<sup>1–4</sup> However, more than 40% of patients experience epiphora within 3–6 months after surgery.<sup>4,5</sup> Some of these undergo secondary or even more surgical reduction to remove the partially transplanted gland.<sup>4,5</sup> In addition, saliva-tears from transplanted submandibular glands show increased sodium level and osmolality, increased lysozyme and amylase levels, and higher protein content than normal saliva.<sup>6</sup> These results suggest that the secretory

function of glands is changed after transplantation. Therefore, elucidation of the secretory mechanism of transplanted submandibular glands is important for developing an effective strategy to control the epiphora after transplantation.

Salivary gland secretion is dependent on a variety of proteins, including receptors, transport proteins, signaling molecules, and enzymes.<sup>7</sup> Proteomic analysis presents a new field of research that can detect potential biomarkers of disease or reveal key factors during the pathophysiological process of the disease. Human whole saliva, parotid saliva, and submandibular-sublingual saliva have been examined by comprehensive proteomics analysis.<sup>8–17</sup> Moreover, proteomic analyses has been used to assess whole saliva, parotid saliva, and parotid glands from patients with Sjögren's syndrome with revealing results.<sup>18–20</sup> Comprehensive analysis of the proteome of submandibular glands has not been performed to date and it has the potential to reveal important information regarding salivary secretory function.

In the present study, we examined proteomic changes in transplanted submandibular glands with hypersecretion by 2-D

**Received:** September 21, 2010

**Published:** March 08, 2011

gel electrophoresis (2-DE) and electrospray ionization quadrupole/time-of-flight mass spectrometry (ESI-Q-TOF-MS/MS) to identify potential key proteins and signaling pathways that play a critical part in the development of epiphora. We also evaluated the role of proteins with altered expression in the hypersecretion of transplanted submandibular glands.

## MATERIALS AND METHODS

### Antibodies

Antibodies to extracellular signal-regulated kinase 1/2 (ERK1/2), phosphorylated ERK1/2 (p-ERK1/2), p38 mitogen-activated protein kinase (p38MAPK), p-p38MAPK, and FITC-, and TRITC-conjugated secondary antibodies were from Santa Cruz Biotechnology (Santa Cruz, CA). Antibodies to c-Jun N-terminal kinase (JNK) and p-JNK were from Cell Signaling Technology (Danvers, MA). Antibody to vimentin was from DakoCytomation (Glostrup, Denmark). Antibody to glyceraldehyde-3-phosphate dehydrogenase (GAPDH) was from Abmart (Shanghai). The anticalponin antibody, antimouse, antirabbit and antigoat IgG horseradish peroxidase (HRP)-conjugated, secondary antibodies were from ZSGB-BIO (Beijing).

### Selection of Subjects and Collection of Submandibular Glands

Human transplanted submandibular gland samples were obtained from 12 patients (aged 19 to 52) who underwent surgical reduction for epiphora within 3 to 12 months after gland transplantation for dry eye. The control samples were from 12 patients (aged 44 to 56) who had primary oral squamous cell carcinoma but had not received irradiation and chemotherapy and were undergoing functional neck dissection as part of surgical treatment. All control glandular tissues were confirmed to be histologically normal. Within 30 min of collection, the submandibular gland samples were transported to the laboratory in 4 °C Krebs–Ringer Hepes (KRH) solution (120 mM NaCl, 5.4 mM KCl, 1 mM CaCl<sub>2</sub>, 0.8 mM MgCl<sub>2</sub>, 11.1 mM glucose, 20 mM Hepes, pH 7.4) aerated with 95% O<sub>2</sub> and were used fresh or stored at –80 °C. The research protocol was approved by the Peking University Institutional Review Board, and prior to tissue collection, all participants signed an informed consent document.

### Protein extraction

The submandibular gland tissue from each patient was minced into small pieces and homogenized in a lysis buffer (7 M urea, 2 M thiourea, 4% (w/v) CHAPS, 65 mM dithiothreitol (DTT), 0.2% (v/v) IPG buffer (pH 3–10)) in the presence of a 1% (v/w) protease inhibitor-cocktail kit (Sigma-Aldrich, St. Louis, MO) by polytron homogenizer. The insoluble molecules were removed by centrifugation at 25 000 × *g*, 4 °C for 1 h, and the supernatant was collected. The protein concentration in each sample was determined by the Bradford method, with bovine serum albumin used as the standard.

### Two-Dimensional Gel Electrophoresis (2-DE)

Human submandibular gland protein (1.2 mg) was dissolved in rehydration buffer (7 M urea, 2 M thiourea, 4% CHAPS, 65 mM DTT, 0.2% Bio-Lyte, 0.001% bromochlorophenol blue) to a final volume of 300 μL and used for 2-DE as previously described.<sup>21</sup> First-dimension isoelectric focusing (IEF) involved use of 17 cm, pH 3–10, linear immobilized pH-gradient gel (IPG) strips (Bio-Rad, Hercules, CA). The IPG strips were rehydrated for 16 h at 20 °C by placing the strips gel-side down and were covered with mineral oil. Then IEF was performed at

20 °C in following steps: 250 V linear for 0.5 h, 1000 V gradient for 1 h, 8000 V linear for 5 h, and 8000 V gradient until 60 000 Vh. After IEF, the IPG strips were equilibrated in buffer containing 6 M urea, 20% glycerol, 0.375 M Tris-HCl (pH 8.8), 2% SDS and 20 mg/mL DTT for 15 min, and then for another 15 min in the same buffer with 25 mg/mL iodoacetamide replacing DTT. The second dimension involved 12% SDS-PAGE gels at 10 mA/gel for 30 min followed by 20 mA/gel until completion.

### Coomassie Brilliant Blue R-250 Staining and Image Analysis

Gels were stained with Coomassie brilliant blue and destained to visualize the protein bands. An amount of 1 g of Coomassie brilliant blue R-250 (Sigma-Aldrich, St. Louis, MO) was dissolved in 200 mL of a mixture of 45% (v/v) methanol, 7.5% (v/v) glacial acetic acid and 47.5% (v/v) water. After gel electrophoresis, gels were rinsed with Milli-Q water and then incubated at room temperature for 1 h in the staining solution. After incubation, the staining solution was removed, and the gel was rinsed with Milli-Q water and then incubated overnight at room temperature in the destaining solution (45% v/v methanol, 7.5% v/v glacial acetic acid, and 47.5% v/v water). The images were analyzed with use of PD-Quest software 8.0.1 (Bio-Rad, Hercules, CA), according to the following: spot detection, spot editing, background subtraction, spot matching and normalization. The resulting data were log-transformed for parametric analyses by use of SPSS 16.0 for Windows (SPSS, Chicago, IL) and Prism 5 software (GraphPad Inc., San Diego, CA).

### In-Gel Digestion

The gel lanes containing the labeled protein sample were excised horizontally into 2-mm-thick bands and washed in 200 μL of 50% acetonitrile (ACN)/50% water twice for 30 min each. The pieces were destained with 200 μL of 30% ACN/100 mM NH<sub>4</sub>HCO<sub>3</sub>, 50% ACN/50 mM NH<sub>4</sub>HCO<sub>3</sub> and 50% ACN/25 mM NH<sub>4</sub>HCO<sub>3</sub> for 3 times at room temperature. Gel pieces were then dried in a Hetovac vacuum centrifuge (HETO, Allerod, Denmark). Dried pieces of gel were rehydrated for 1 h at 4 °C in 10 μL of a solution of trypsin (Promega, Southampton, U.K.) at 20 ng/μL, and then 20 μL of 25 mM NH<sub>4</sub>HCO<sub>3</sub> was added. After overnight incubation at 37 °C, gel pieces were dried in a high-vacuum centrifuge before being rehydrated by the addition of 50 μL H<sub>2</sub>O. Elution of the peptides involved 50 μL of 60% ACN/5% trifluoroacetic acid (TFA) for 15 min at room temperature with occasional shaking. The TFA solution containing the proteins was transferred to a polypropylene tube with 5 μL of 60% ACN/5% TFA. A second elution of the peptides was performed with 50 μL of 5% TFA in 60% ACN for 15 min at room temperature with occasional shaking. The second TFA solution was pooled with the first one. The volume of the pooled extracts was reduced to 1–2 μL by evaporation under vacuum. Before mass spectrometry (MS), the volumes of peptide containing solutions were adjusted to 10 μL by the addition of 0.1% TFA in 60% ACN.

### Protein Identification by ESI-Q-TOF-MS/MS

After the selected protein spots were excised from the gels for decolorization, in-gel digestion, and ESI-Q-TOF-MS/MS (Waters, USA) was performed to identify the selected protein spots.<sup>21</sup> The peptide mixture was analyzed on a Waters Capillary liquid chromatography system including 3 pumps A, B and C (Waters). Fused silica tubing (75 μm × 100 mm) packed with symmetry 300 C<sub>18</sub>, 3.5-μm spherical particles with pore diameter 100 Å (Waters). The flow rate was set at 2.5 μL/min. Samples were

injected at a flow rate of 20  $\mu\text{L}/\text{min}$  with pump C and salts were removed on the precolumn of (0.35  $\times$  5 mm) packed with symmetry 300 C<sub>18</sub>, 3.5- $\mu\text{m}$  spherical particles with pore diameter 100 Å (Waters). The precolumn was connected in the 10-port switching valve and switched to the analytical column after the sample was desalted. Mobile phase A consisted of water/ACN (95/5, v/v) with 0.1% aqueous formic acid (FA). Mobile phase B consisted of water/ACN (5/95, v/v) with 0.1% FA. The separation was performed by running on gradient: 3% B, for 0.1–3.5 min for injection; 5–40% B, for 3.5–40 min; 40–60% B, for 40–60 min; 60–90% B, for 60–65 min; 90–5% B, for 65–70 min; 5–5% B, for 70–90 min. The Cap LC is coupled online with a Q-TOF Ultima Global mass spectrometer (Waters) for detection and protein identification. Peptide mixtures were dissolved with 2  $\mu\text{L}$  of 0.1% FA and injected by the atmosphere on the precolumn with use of a Cap LC system. Peptides were directly eluted into a Q-TOF mass spectrometer (Q-TOF Ultima Global mass spectrometer; Waters) at 250 nL/min on the analytical column. After being analyzed by Mass Lynx 4.0, the data resulting from the MS/MS analysis underwent identification with MASCOT search engine (<http://www.matrixscience.com/>). The parameters were database of Swiss-Port, taxonomy of *Homo sapiens* (human), trypsin of the digestion enzyme, one missed cleavage site, fixed modifications of carbamidomethyl (C), variable modifications of oxidation (M), peptide tolerance of 0.2 Da, MS/MS tolerance of 0.1 Da.

### Submandibular Gland Tissue Preparation

The fresh gland samples obtained from functional neck dissection were minced into small pieces (0.5 mm<sup>3</sup>) as reported previously.<sup>22</sup> The minced samples were cultured at 37 °C for 10 min in Dulbecco's modified Eagle's medium (containing 100 U/mL penicillin and 100  $\mu\text{g}/\text{mL}$  streptomycin) (Gibco; Grand Island, NY) at 37 °C in a humidified atmosphere of 5% CO<sub>2</sub> and 95% air with or without carbachol, PD98059 or U0126 stimulation (all from Sigma-Aldrich, St. Louis, MO). Then the tissues were collected for Western blot analysis and immunofluorescence staining.

### Western Blot Analysis

The protein extracts (20  $\mu\text{g}$ ) derived from each sample were separated on 9% SDS-PAGE and electroblotted on polyvinylidene fluoride membranes as previously described.<sup>23</sup> Nonspecific binding was blocked with 5% nonfat milk in TBS-T (20 mM Tris, 137 mM NaCl, 0.1% Tween-20, pH 7.4) for 2 h at room temperature. Blocked membranes were incubated overnight at 4 °C with antibodies for p-ERK1/2 (1:800), ERK1/2 (1:800), p-p38MAPK (1:800), p38MAPK (1:800), p-JNK (1:1000), JNK (1:1000), vimentin (1:1000) and actin (1:1000). Anti-GAPDH antibody (1:5000) was used as a loading control. The membranes were then probed with HRP-conjugated secondary antibodies (1:4000–8000) at room temperature for 1 h. Immunoreactive protein bands were visualized by use of an enhanced chemiluminescence detection system (GE Biosciences, Buckinghamshire, England) according to the manufacturer's protocol. Densitometry data were analyzed by Quantity One (Bio-Rad, Hercules, CA).

### Immunofluorescence Staining

Gland tissues were sectioned 5- $\mu\text{m}$  thick and fixed in cold acetone for 15 min. After a washing with PBS (137 mM NaCl, 2.7 mM KCl, 4.3 mM Na<sub>2</sub>HPO<sub>4</sub>, 1.4 mM KH<sub>2</sub>PO<sub>4</sub>, pH 7.4) for 3 times, tissue slides were blocked with 20% rabbit serum for 30 min, immunostained with antivimentin (1:100) or anticalponin

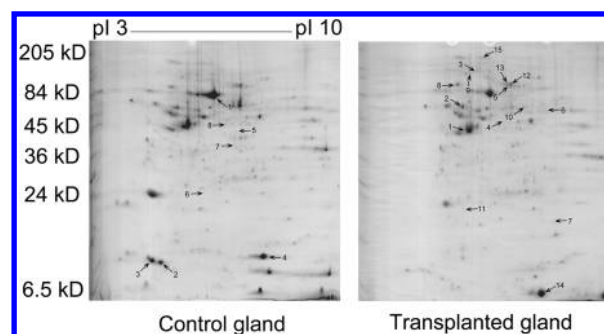


**Figure 1.** Representative 2-D electrophoresis (2-DE) proteome maps of differentially expressed proteins in control and transplanted submandibular glands. Replicate 2-DE gels ( $n = 6$ ) of both control and transplanted glands revealed a total of 23 protein spots differentially expressed. Among them, 8 protein spots downregulated are shown with arrows on the control gland gel, and 15 protein spots upregulated are shown with arrows on the transplanted gland gel.

(1:100) antibodies overnight at 4 °C, and then incubated with TRITC-conjugated secondary antibodies (1:200) for 1 h. Filamentous actin (F-actin) was stained with Alexa Fluor 488-conjugated phalloidin (Sigma-Aldrich, St. Louis, MO) at 37 °C for 1 h according to the manufacturer's instructions. After a washing with PBS for 3 times, nuclei were labeled with 4, 6-diamidino-2-phenylindole (DAPI). Sections were examined under a confocal microscope (Leica TCS SP5, Heidelberg, Germany). The quantitative measurement of F-actin involved Leica TCS SP5 (LAS AF). The fluorescence intensities of F-actin in 9 randomly selected acini in each section from 6 control and transplanted glands were averaged. Data were reported as the total intensity of F-actin in each acinus, the F-actin intensity in apical and lateral areas of acini, and their ratio.

### Statistical Analysis

Statistical analysis of 2 groups involved unpaired Student's *t*-test and more than 2 groups one-way ANOVA followed by Bonferroni's post hoc test. Data were presented as means  $\pm$  SD  $P < 0.05$  was considered statistically significant.

## RESULTS

### 2-DE Analysis of Transplanted Submandibular Glands

To examine the alteration of protein expression in transplanted glands, whole tissue extracts were prepared and analyzed by 2-DE. Representative gels of control and transplanted tissue extracts are in Figure 1. 2-DE with loading of an equal amount of total protein (1.2 mg/gel) revealed approximately 550 protein spots in each 2-D gel. All gel spots showing significantly changed abundance were then highlighted and checked manually to eliminate any artifacts due to gel distortions, inappropriately matched or mistakenly detected spots. Differential analysis comparing replicate 2-DE gels ( $n = 6$ ) of both control and transplanted glands revealed 23 protein spots with at least 2-fold difference in abundance ( $P < 0.05$ ), of which 8 proteins demonstrated decreased abundance (Figure 1; control gland arrows), and other 15 increased abundance (Figure 1; transplanted gland arrows).

### Protein Identification

To identify the protein spots with changed expression, the differentially expressed spots were excised from gels, then underwent in-gel digestion with trypsin, and were identified by ESI-Q-TOF-MS/MS. Information on the proteins with changed

Table 1. Upregulated Proteins in Transplanted Glands Compared with Control Glands

spot no.	protein name	access number	score	queries matched	coding gene	cellular component	molecular function
1	Actin, cytoplasmic 1	P60709	777	27	<i>ACTB</i>	Cytoskeleton NuA4 histone acetyltransferase complex, histone methyltransferase complex	ATP binding, nitric-oxide synthase binding, structural constituent of cytoskeleton
2	Vimentin	P08670	1144	43	<i>VIM</i>	Cytoplasm, intermediate filament	Protein binding, structural constituent of cytoskeleton,
3	Alpha-actinin-4	O43707	170	13	<i>ACTN4</i>	Nucleolus, perinuclear region of cytoplasm, protein complex, pseudopodium	Actin filament binding, calcium ion binding, integrin binding, nucleoside binding, protein homodimerization activity
4	Keratin, type I cytoskeletal 23	Q9C075	154	14	<i>KRT23</i>	Intermediate filament	Structural molecule activity
5	lamin-A/C	P02545	429	18	<i>LMNA</i>	Cytoplasm Intermediate filament, nucleus, plasma membrane	Protein binding, structural molecule activity
6	Glutathione reductase	P00390	71	5	<i>GSR</i>	Metabolism Cytosol, mitochondrion	FAD binding, NADP or NADPH binding, electron carrier activity, glutathione-disulfide reductase activity
7	Flavin reductase	P30043	609	22	<i>BLVRB</i>	Cytoplasm	Biliverdin reductase activity, coenzyme binding, flavin reductase activity
8	78 kDa glucose-regulated protein	P11021	1222	79	<i>HSPA5</i>	ER-Golgi intermediate compartment, cell surface, endoplasmic reticulum lumen, integral to endoplasmic reticulum membrane, melanosome, nucleus, perinuclear region of cytoplasm	ATP binding, calcium ion binding, caspase inhibitor activity, protein binding and bridging, unfolded protein binding
9	Transitional endoplasmic reticulum ATPase	P55072	65	10	<i>VCP</i>	Cytosol, endoplasmic reticulum, microsome, nucleus	ATP binding, ATPase activity, lipid binding, protein domain specific binding
10	Cytosol aminopeptidase	P68767	327	27	<i>RNPEP</i>	Protein hydrolysis and degradation	Aminopeptidase activity, magnesium ion binding, manganese ion binding, metalloexopeptidase activity, zinc ion binding
11	Cathepsin B	P07858	188	6	<i>CTSB</i>	Lysosome, melanosome Molecular transport	Cysteine-type endopeptidase activity
12	Serotransferrin	P02787	582	39	<i>TF</i>	Endocytic vesicle, mitochondrion	Ferric iron binding
13	Serotransferrin	P02787	370	21	<i>TF</i>	Endocytic vesicle, mitochondrion	Ferric iron binding
14	Hemoglobin subunit beta	P68871	1272	64	<i>Hbb-b2</i>	Hemoglobin complex	Heme binding, hemoglobin binding, oxygen binding, oxygen transporter activity
15	Collagen alpha-2(VI) chain	P12110	85	12	<i>COL6A2</i>	Cell—cell adhesion Cytoplasm, extracellular space, proteinaceous extracellular matrix	Extracellular matrix structural constituent, protein binding, bridging

**Table 2. Down-regulated Proteins in Transplanted Glands Compared with Control Glands**

spot no.	protein name	access number	score	queries matched	coding gene	cellular component	molecular function
Secretion proteins							
1	Alpha-amylase 1	P04745	621	24	AMY1A	Extracellular region	Alpha-amylase activity, calcium ion binding, chloride ion binding, protein binding
2	Cystatin-S	P01036	1179	84	CST4	Extracellular region	cysteine-type endopeptidase inhibitor activity
3	Cystatin-SA	P09228	200	17	CST2	Extracellular region	Cysteine-type endopeptidase inhibitor activity
4	Cystatin-SN	P01037	685	42	CST1	Extracellular region	Cysteine-type endopeptidase inhibitor activity
Metabolism							
5	Short-chain specific acyl-CoA dehydrogenase	P16219	92	8	ACADS	Mitochondrial matrix	FAD binding, butyryl-CoA dehydrogenase activity, electron carrier activity
Protein hydrolysis and degradation							
6	Proteasome subunit beta type-4	P28070	121	7	PSMB4	Centrosome, cytosol, nucleus, proteasome core complex	Threonine-type endopeptidase activity
Protein biosynthesis							
7	Delta-aminolevulinic acid dehydratase	P13716	244	17	ALAD	Cytosol	Porphobilinogen synthase activity, zinc ion binding
Visual perception							
8	Ornithine aminotransferase	P04181	133	11	OAT	Mitochondrial matrix	Ornithine-oxo-acid transaminase activity, protein binding, pyridoxal phosphate binding

expression are summarized in Tables 1 and 2 according to information collected on Swiss-Prot (<http://expasy.org/sprot/>). Among the differentially expressed proteins, 5 proteins were involved in cytoskeleton (ACTB, VIM, ACTN4, KRT23, LMNA), 5 were related to metabolism (GSR, BLVRB, HSPA5, VCP, ACADS), 4 were secretory proteins (AMY1A, CST4, CST2, CST1), 3 participated in protein hydrolysis and degradation (RNPEP, CTSB, PSMB4), 3 were involved in molecular transport (TF; TF; Hbb-b2), and COL6A2, ALAD and OAT were related to cell–cell adhesion, protein biosynthesis and visual perception, respectively. Interestingly, the cytoskeletal proteins, accounting for 21.7% of the differentially expressed proteins, were all upregulated and the secretory proteins were all down-regulated in transplanted glands. Finally, the expression of proteins involved in molecular transport was consistently increased in transplanted glands.

#### Validation of Actin and Vimentin Upregulation in Transplanted Glands

Cytoskeletal proteins play important roles in both intracellular transport and cellular division. In the present study, 5 differentially expressed cytoskeletal proteins were all upregulated in transplanted submandibular glands. To confirm the data obtained from 2-DE, we measured protein contents of actin and vimentin as representative cytoskeletal proteins in additional independent samples from control and transplanted glands. Western blot analysis revealed the concentrations of actin and vimentin in transplanted gland increased by 54.2% and 53.2%, respectively, as compared with controls (Figure 2) ( $0.91 \pm 0.15$  vs  $0.59 \pm 0.06$ ,  $P < 0.05$ ;  $1.18 \pm 0.08$  vs  $0.77 \pm 0.07$ ,  $P < 0.05$ ), which were essentially in agreement with 2-DE results.

#### Distribution of Vimentin and F-Actin in Transplanted Glands

To evaluate the possible effect of the increased level of cytoskeletal proteins, we next established the localization of vimentin and F-actin, a polymerized form of actin, in transplanted submandibular glands by confocal microscopy. Vimentin is one of the markers of myoepithelial cells and is also expressed in mesenchymal cells. In control glands, the distribution of vimentin

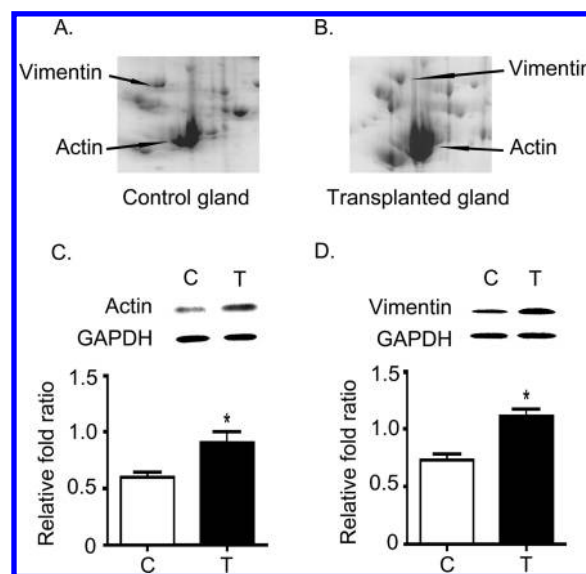


**Figure 2.** Expression of vimentin and actin in control and transplanted submandibular glands. (A) and (B) Representative 2-DE images of vimentin and actin in control and transplanted glands. (C) and (D) Western blot analysis of actin and vimentin expression. Quantification was normalized to GAPDH expression. C, control gland; T, transplanted gland. Values are means  $\pm$  SD from 6 independent experiments. \*  $P < 0.05$  compared with control gland.

was around acini and ducts and less in mesenchyme (Figure 3A). However, in transplanted glands, the positive staining of vimentin was increased and mainly distributed in mesenchyme (Figure 3B). To confirm whether the increase in vimentin in transplanted glands was related to myoepithelial cells, we further detected the distribution of calponin, a specific marker of myoepithelial cells.<sup>24</sup> Calponin was located tightly around the acini in control glands (Figure 3C), which was consistent with the subcellular location of calponin in cells in previous reports.<sup>24</sup> The distribution of calponin in transplanted glands was similar to

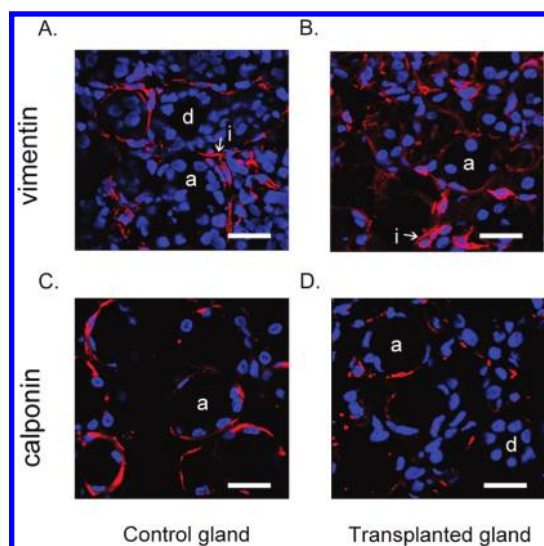


**Figure 3.** Distribution of vimentin and calponin in control and transplanted glands. Submandibular gland tissues were sectioned, fixed, and incubated with antivimentin or anticalponin antibodies, then stained with a TRITC-conjugated secondary antibody. Nuclei were stained with DAPI (blue). (A) and (B) Distribution of vimentin (red) in control and transplanted submandibular glands by confocal microscopy. (C) and (D) Distribution of calponin (red) in control and transplanted glands. a, acinus; d, duct; i, interstitial cell. Bar: 25  $\mu\text{m}$ .

that in controls (Figure 3D), which suggests that increased vimentin was mainly located in interstitial fibroblast cells.

We next detected the distribution of F-actin, a polymerized form of actin. In control glands, F-actin staining was detected in cytoplasm close to apical and lateral membranes of acinar cells, with continuous and uniform distribution, and in cytoplasm close to the basal membrane of acinar cells, with discontinuous positive staining (Figure 4A). However, in transplanted glands, F-actin distribution was decreased in apical and lateral cytoplasm and was aggregated discontinuously in basal cytoplasm of acinar cells (Figure 4B). The intensity of total F-actin in acinar cells and around the acini of transplanted glands was not significantly different from that of control glands ( $29.89 \pm 8.54$  vs  $26.65 \pm 6.21$ ) (Figure 4C). However, the intensity of F-actin in apical and lateral cytoplasm of acinar cells of transplanted glands was 37.2% lower than that of control glands ( $16.08 \pm 5.80$  vs  $25.61 \pm 4.53$ ;  $P < 0.01$ ) (Figure 4D). The ratio of F-actin in apical and lateral cytoplasm to total F-actin of each acinus in transplanted glands reduced by 35.8% compared with that in control glands ( $0.59 \pm 0.24$  vs  $0.92 \pm 0.27$ ,  $P < 0.01$ ) (Figure 4E).

#### Expression of MAPK in Transplanted Glands

The MAPK signaling pathway modulates the transcription and function of a large number of proteins by phosphorylation. To test whether MAPK level was changed in transplanted glands, we examined the phosphorylation of ERK1/2, p38MAPK and JNK by Western blot analysis. p-ERK1/2 was increased by 85.0% in transplanted glands as compared with control glands ( $1.61 \pm 0.13$  vs  $0.87 \pm 0.16$ ,  $P < 0.01$ ; Figure 5A). However, the phosphorylation of p38MAPK and JNK did not differ between control and transplanted glands (Figure 5B and C).

#### Effect of Carbachol on p-ERK1/2 and Redistribution of F-Actin

Carbachol, an agonist of muscarinic cholinergic receptor, can significantly increase fluid and electrolyte secretion from salivary

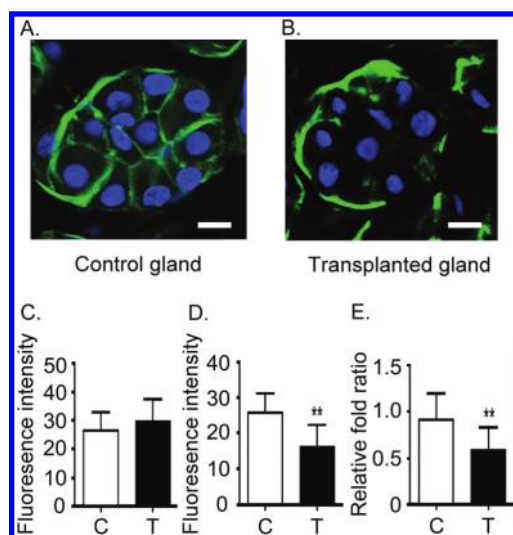


**Figure 4.** Distribution of F-actin in control and transplanted glands. F-actin was stained with Alexa Fluor 488-conjugated phalloidin. Nuclei were stained with DAPI (blue). (A) and (B) Distribution of F-actin (green) in control and transplanted glands by confocal microscopy. Bar: 8  $\mu\text{m}$ . Quantitative detection of F-actin in 9 randomly selected acini in each section from 6 control and transplanted glands. (C) Fluorescence intensity of total F-actin in each acinus. (D) Fluorescence intensity of F-actin in apical and lateral cytoplasm of acinar cells. (E) Ratio of F-actin in apical and lateral cytoplasm of acinar cells to total F-actin. C, control gland; T, transplanted gland. Values are means  $\pm$  SD from 6 independent experiments. \*\*  $P < 0.01$ .

glands. To further investigate the possible effects of ERK1/2 activation and redistribution of F-actin on the secretion of submandibular glands, we used carbachol (10  $\mu\text{M}$ ) to stimulate the cultured human submandibular gland tissues for 10 min, and then performed Western blot analysis and immunofluorescence staining. In control glands, the basic level of p-ERK1/2 was weak. The level of p-ERK1/2 was significantly increased, by 47.3%, after carbachol incubation for 10 min ( $1.37 \pm 0.15$  vs  $0.93 \pm 0.07$ ,  $P < 0.01$ ; Figure 5D). Preincubation gland tissues with PD98059 (20  $\mu\text{M}$ , 30 min), an inhibitor of ERK upstream kinase, or U0126 (5  $\mu\text{M}$ , 30 min), an inhibitor of ERK, the carbachol-induced increase in p-ERK1/2 was suppressed, whereas PD98059 or U0126 alone had no effect on the expression of basic p-ERK1/2 (Figure 5D). The results suggested that ERK1/2 was activated in carbachol-induced hypersecretive submandibular glands.

In the unstimulated control gland, the distribution of F-actin was located in apical, lateral and basal cytoplasm of acinar cells (Figure 6A). However, after carbachol stimulation for 10 min, F-actin was significantly decreased in apical and lateral cytoplasm of acinar cells and aggregated discontinuously in the basal cytoplasm of acinar cells (Figure 6B), a pattern similar to that observed in transplanted submandibular glands (Figure 4B). Preincubation with PD98059 (20  $\mu\text{M}$ , 30 min) or U0126 (5  $\mu\text{M}$ , 30 min) inhibited the carbachol-induced redistribution of F-actin (Figure 6D and F), whereas PD98059 or U0126 alone had no effect on the distribution of F-actin (Figure 6C and E). Quantitative analysis showed that the intensity of F-actin in apical and lateral cytoplasm of acinar cells in carbachol-stimulated glands was significantly lower, by 45.0%, than that of unstimulated glands ( $14.08 \pm 4.50$  vs  $25.61 \pm 4.53$ ;  $P < 0.01$ ; Figure 6G). The ratio of F-actin in apical and lateral cytoplasm to

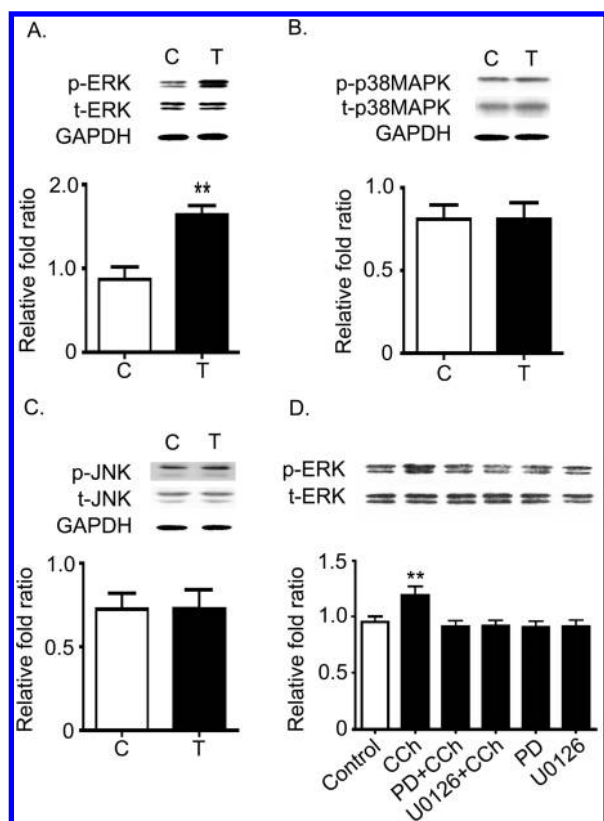


**Figure 5.** Expression of mitogen-activated protein kinase (MAPK) in submandibular glands. Protein extracts from control and transplanted glands were immunoblotted with antibodies specific for phosphorylated ERK1/2 (p-ERK1/2) (A), p-p38MAPK (B) and p-JNK (C). Normalization was to total ERK1/2, p38MAPK, JNK and GAPDH, respectively. C, control gland; T, transplanted gland. Values are means  $\pm$  SD from 6 independent experiments. \*\*  $P < 0.01$  compared with control glands. (D) Phosphorylation of ERK1/2 in carbachol-treated submandibular glands. Quantification involved normalization to total ERK1/2. Control, control gland; CCh, carbachol (10  $\mu$ M) treatment for 10 min; PD + CCh, pretreatment with 20  $\mu$ M PD98059 for 30 min, then stimulation with carbachol for 10 min; U0126 + CCh, pretreatment with 5  $\mu$ M U0126 for 30 min, then stimulation with carbachol for 10 min; PD, treatment with 20  $\mu$ M PD98059 for 30 min; U0126, treatment with 5  $\mu$ M U0126 for 30 min. Values are means  $\pm$  SD from 6 independent experiments. \*\*  $P < 0.01$  compared with control.

total F-actin of each acinus in carbachol-stimulated glands reduced by 32.6% compared with unstimulated glands ( $0.62 \pm 0.33$  vs  $0.92 \pm 0.27$ ,  $P < 0.01$ ; Figure 6H). Other groups were no difference compared with control. These results suggested that carbachol induced the redistribution of F-actin in an ERK1/2-dependent manner and ERK1/2 phosphorylation and redistribution of F-actin might be involved in hypersecretion of submandibular glands.

## DISCUSSION

The present study first time compared the protein expression in the submandibular glands of epiphora patients and the control subjects. The results show that the expression of 23 proteins in the glands of epiphora patients was significantly changed. Amylase is a major enzyme of saliva and cystatins are present in saliva and are involved in the regulation of protein degradation at sites of

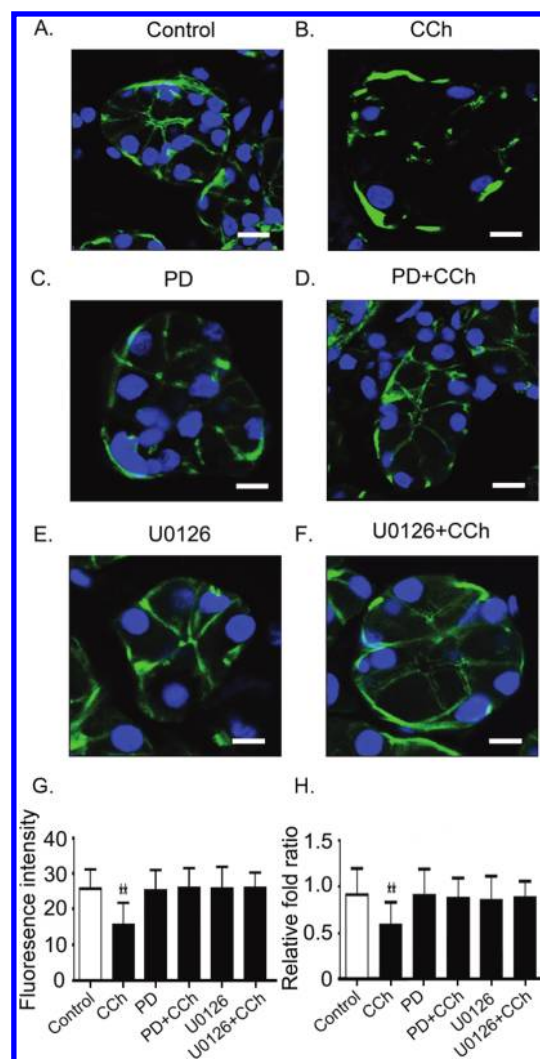


**Figure 6.** Distribution of F-actin in carbachol-treated submandibular glands. F-actin was stained with Alexa Fluor 488-conjugated phalloidin; nuclei were stained with DAPI (blue). (A) Representative image of F-actin in control gland. (B) F-actin staining after 10  $\mu$ M carbachol treatment for 10 min. (C) F-actin staining after 20  $\mu$ M PD98059 for 30 min. (D) Pretreatment with 20  $\mu$ M PD98059, then stimulation with carbachol for 10 min. (E) F-actin staining after 5  $\mu$ M U0126 for 30 min. (F) Pretreatment with 5  $\mu$ M U0126, then stimulation with carbachol for 10 min. Bar: 8  $\mu$ m. Quantitative detection of F-actin in 9 randomly selected acini in each section from 6 independent experiments. (G) Fluorescence intensity of F-actin in apical and lateral cytoplasm of acinar cells. (H) Ratio of F-actin in apical and lateral cytoplasm of acinar cells to total F-actin. Values are means  $\pm$  SD from 6 independent experiments. \*\*  $P < 0.01$ .

inflammation or microbial infection.<sup>25</sup> Among them, the S-type cystatin (cystatin S, SA and SN) is a main product of submandibular-sublingual glands.<sup>26</sup> Due to their importance in the salivary glands, their expression in the glands of epiphora patients may shed light on the mechanism of the hypersecretion after transplantation. We found that the expression of 4 secretory proteins (alpha-amylase, cystatin S, SA and SN) was decreased in epiphora glands. It has been reported that the activity of alpha-amylase in the saliva-tear from patients with submandibular gland transplantation was increased,<sup>6</sup> the alpha-amylase activity in saliva was increased and the content of alpha-amylase protein

decreased in the submandibular gland after isoproterenol perfusion in rabbit,<sup>27</sup> and carbachol-stimulated secretion of S<sub>1</sub>, S<sub>2</sub> (2 forms of cystatin S phosphorylation) and SN was increased in human submandibular glands.<sup>28</sup> Thus, the results of the present study suggest that the hypersecretion of the transplanted submandibular glands is not mediated by the changes in the expression of these secretory proteins.

The expression of 4 proteins involved in metabolism (glutathione reductase, flavin reductase, transitional endoplasmic reticulum ATPase, and 78 kDa glucose-regulated protein) was upregulated in the glands of epiphora patients. It has been reported that the activity of glutathione reductase is increased in rat parotid saliva after isoproterenol stimulation, indicating that the enzyme may play a part in salivary secretion or is a target of sympathetic stimulation. More importantly, it also has been demonstrated that the changed glutathione metabolism is involved in exocytosis, endocytosis, membrane recycling, increased amino acid transport, and resynthesis of secretory proteins.<sup>29</sup> Therefore, overexpression of metabolism-related proteins observed in the present study is expected to be related to the increased secretion of transplanted submandibular glands in patients with epiphora. The accurate mechanisms by which the overexpressed metabolism-related proteins mediate the hypersecretion in the glands of epiphora patients needs further investigation in our laboratory.

Of the cytoskeletal proteins, actin is a major structural element of cytoskeleton and is involved in saliva secretion.<sup>30–32</sup> Alpha-actinin-4 is an actin-binding protein and is present in the perinuclear region of cytoplasm and nucleus and colocalized with actin stress fibers.<sup>33</sup> Vimentin, keratin and lamin-A/C are components of intermediate filaments. Vimentin is one of the markers of myoepithelial cells and also expressed in interstitial fibroblast cells.<sup>24</sup> The contraction of myoepithelial cells helps in secretion by compressing the underlying parenchyma.<sup>24</sup> Since the cytoskeleton is essential to maintain cell shape, protect the cell, enable cellular motion, and play important roles in both intracellular transport and cellular division,<sup>34,35</sup> we further evaluated the possible effects of vimentin and actin on secretion of the transplanted submandibular gland from patients with epiphora. Using proteomic analysis, Western blot and immunofluorescence staining, we demonstrated that vimentin was upregulated in transplanted glands, and the increased vimentin was mainly located in interstitial fibroblast cells in transplanted glands. Distribution of calponin, a specific marker for myoepithelial cells, also confirmed that increased vimentin level in transplanted gland was mainly in mesenchyme. These results are consistent with previous study that the connective tissue is increased after submandibular gland transplantation.<sup>5</sup> However, there is no evidence indicating that the increased vimentin level is directly involved in the excessive secretion of transplanted glands.

The individual subunits of actin (monomers) are known as globular actin (G-actin). G-actin subunits assemble into long filamentous polymers called F-actin. Under physiological conditions, G-actin readily polymerizes to form F-actin, with concomitant hydrolysis of ATP. The polymerization and depolymerization of actin filaments generates direct forces that drive changes in cell shape and, together with molecular motors that move along the actin filaments and microtubules, guide the organization of cellular components.<sup>34</sup> The disruption of microfilaments with cytochalasin B prevented amylase release in rat submandibular glands, which indicates that secretion of amylase depends on the integrity of microfilaments.<sup>31,32</sup> It has been reported that actin filament integrity was required for the activation of Cl<sup>-</sup> channels

in rat parotid acinar cells.<sup>32</sup> The optimal Na<sup>+</sup>/H<sup>+</sup> exchanger activity also requires the integrity of the cellular F-actin network in a hamster ovary cell line.<sup>36</sup> However, actin cytoskeleton also exerted an inhibiting effect on CIC-2 chloride channel, and disruption of actin cytoskeleton led to the activation of CIC-2 chloride channel in *Xenopus* oocytes.<sup>30</sup> The exact role of the polymerization and depolymerization of actin filaments in saliva secretion remains unclear. In the present study, the content of actin was increased in transplanted submandibular glands, but the expression of F-actin, a polymerized form of actin, was not significantly increased in acinar cells. More importantly, quantitative analysis revealed that F-actin in apical and lateral cytoplasm was significantly decreased in transplanted glands. These results suggest that depolymerization of actin filaments in apical and lateral cytoplasm was accelerated in the transplanted gland, and might explain, at least in part, the increased expression of actin in the transplanted gland measured by proteomic analysis and Western blot analysis. Our results also showed that F-actin staining was more discontinuous and aggregated in basal cytoplasm of acini in the glands of epiphora patients, which suggests that polymerization and depolymerization of actin filaments and their subcellular distribution are likely to be involved in hypersecretion in transplanted submandibular gland.

Since fluid secretion in salivary glands is mainly controlled by muscarinic receptors, we tested whether the muscarinic agonist carbachol induces redistribution of actin filaments in transplanted submandibular glands. We found that the pattern of F-actin redistribution in response to carbachol-stimulated submandibular gland tissues was similar to that in transplanted glands, characterized by decreased F-actin in apical and lateral cytoplasm and aggregated F-actin in basal cytoplasm of acinar cells. In resting parotid acinar cells, the cytoskeletal protein fodrin and actin appeared as a continuous ring under the plasma membrane of most cells, which disappeared almost completely upon stimulation with secretagogues, these cytoskeletal changes occurred in parallel with amylase secretion.<sup>37</sup> In human labial salivary glands, F-actin was located in the apical and basolateral area of acinar cells, but in the hyposalivatory gland of Sjögren's syndrome patients, F-actin was redistributed in cytoplasm, except the apical region and basolateral cortex.<sup>38</sup> Taken together, these results suggest that a reorganization of F-actin might play an essential role in regulation of saliva secretion. Because myoepithelial cells also contain F-actin filaments and they surround the acini tightly, separating F-actin in the basal cytoplasm of acinar cells from myoepithelial cells is difficult. The possibility of F-actin redistribution in myoepithelial cells to stimulate salivation cannot be excluded.

ERK plays a critical role in intracellular signal transduction. Activation of ERK1/2 is also linked to muscarinic-responsive NaHCO<sub>3</sub> cotransport activity in kidney cells and mucin secretion in conjunctival goblet cells and may negatively regulate carbachol-stimulated Cl<sup>-</sup> secretion in colonic epithelial cells.<sup>39–41</sup> Activation of MEK/ERK signaling pathway induces disruption of the actin cytoskeleton in rat fibroblasts but not in human fibroblasts.<sup>42</sup> However, in salivary gland, whether phosphorylation of ERK1/2 participates in redistribution of F-actin is unknown. One of our previous studies indicates that carbachol increased the expression of p-ERK1/2 and promoted secretion in transplanted rabbit submandibular glands and cultured acinar cells.<sup>43</sup> In the present study, we found the expression of p-ERK1/2 increased in transplanted glands of epiphora patient and also in carbachol-stimulated submandibular glands. Inhibition of p-ERK1/2 suppressed

the carbachol-stimulated redistribution of F-actin in the control glands. These results suggest that phosphorylation of the intracellular signaling protein ERK1/2 may be responsible for the redistribution of F-actin in the hypersecretive human submandibular glands. The accurate mechanism of ERK1/2 phosphorylation mediated F-actin redistribution in gland secretion needs to be further studied.

In summary, the present study provides a comprehensive proteomic analysis of putative key regulators in hypersecretive transplanted submandibular glands. Increased secretion in transplanted submandibular glands is associated with a marked reorganization of F-actin in an ERK1/2-dependent manner. These findings will help better understand the molecular mechanisms of transplanted submandibular glands and provide a basis for finding new therapeutic strategies to control epiphora after gland transplantation.

## AUTHOR INFORMATION

### Corresponding Author

\*Dr. Li-Ling Wu, Department of Physiology and Pathophysiology, Peking University Health Science Center, Beijing 100191, China. Phone: 86-10-82802403. Fax: 86-10-82802403. E-mail: pathophy@bjmu.edu.cn. Dr. Guang-Yan Yu, Department of Oral and Maxillofacial Surgery, Peking University School and Hospital of Stomatology, Beijing 100081, China. Phone: 86-10-62191099. Fax: 86-10-62173402. E-mail: gyyu@263.net.

## ACKNOWLEDGMENT

This study was supported by grants from the National Natural Science Foundation of China (Nos. 30730102, 30700949 and 30973316) and the National Support Program for Science and Technology (No. 2007BAI18B11)

## REFERENCES

- (1) Sieg, P.; Geerling, G.; Kosmehl, H.; Lauer, I.; Warnecke, K.; von Domarus, H. Microvascular submandibular gland transfer for severe cases of keratoconjunctivitis sicca. *Plast. Reconstr. Surg.* **2000**, *106* (3), 554–60.
- (2) Geerling, G.; Sieg, P.; Bastian, G. O.; Laqua, H. Transplantation of the autologous submandibular gland for most severe cases of keratoconjunctivitis sicca. *Ophthalmology* **1998**, *105* (2), 327–35.
- (3) Murube-del-Castillo, J. Transplantation of salivary gland to the lacrimal basin. *Scand. J. Rheumatol. Suppl.* **1986**, *61*, 264–7.
- (4) Yu, G. Y.; Zhu, Z. H.; Mao, C.; Cai, Z. G.; Zou, L. H.; Lu, L.; Zhang, L.; Peng, X.; Li, N.; Huang, Z. Microvascular autologous submandibular gland transfer in severe cases of keratoconjunctivitis sicca. *Int. J. Oral Maxillofac. Surg.* **2004**, *33* (3), 235–9.
- (5) Geerling, G.; Garrett, J. R.; Paterson, K. L.; Sieg, P.; Collin, J. R.; Carpenter, G. H.; Hakim, S. G.; Lauer, I.; Proctor, G. B. Innervation and secretory function of transplanted human submandibular salivary glands. *Transplantation* **2008**, *85* (1), 135–40.
- (6) Geerling, G.; Honnicke, K.; Schroder, C.; Framme, C.; Sieg, P.; Lauer, I.; Pagel, H.; Kirschstein, M.; Seyfarth, M.; Marx, A. M.; Laqua, H. Quality of salivary tears following autologous submandibular gland transplantation for severe dry eye. *Graefes Arch. Clin. Exp. Ophthalmol.* **2000**, *238* (1), 45–52.
- (7) Melvin, J. E.; Yule, D.; Shuttleworth, T.; Begenisich, T. Regulation of fluid and electrolyte secretion in salivary gland acinar cells. *Annu. Rev. Physiol.* **2005**, *67*, 445–69.
- (8) Ghafouri, B.; Tagesson, C.; Lindahl, M. Mapping of proteins in human saliva using two-dimensional gel electrophoresis and peptide mass fingerprinting. *Proteomics* **2003**, *3* (6), 1003–15.
- (9) Vitorino, R.; Lobo, M. J.; Ferrer-Correia, A. J.; Dubin, J. R.; Tomer, K. B.; Domingues, P. M.; Amado, F. M. Identification of human whole saliva protein components using proteomics. *Proteomics* **2004**, *4* (4), 1109–15.
- (10) Wilmarth, P. A.; Riviere, M. A.; Rustvold, D. L.; Lauten, J. D.; Madden, T. E.; David, L. L. Two-dimensional liquid chromatography study of the human whole saliva proteome. *J. Proteome Res.* **2004**, *3* (5), 1017–23.
- (11) Hu, S.; Xie, Y.; Ramachandran, P.; Ogorzalek Loo, R. R.; Li, Y.; Loo, J. A.; Wong, D. T. Large-scale identification of proteins in human salivary proteome by liquid chromatography/mass spectrometry and two-dimensional gel electrophoresis-mass spectrometry. *Proteomics* **2005**, *5* (6), 1714–28.
- (12) Amado, F. M.; Vitorino, R. M.; Domingues, P. M.; Lobo, M. J.; Duarte, J. A. Analysis of the human saliva proteome. *Expert Rev. Proteomics* **2005**, *2* (4), 521–39.
- (13) Xie, H.; Rhodus, N. L.; Griffin, R. J.; Carlis, J. V.; Griffin, T. J. A catalogue of human saliva proteins identified by free flow electrophoresis-based peptide separation and tandem mass spectrometry. *Mol. Cell. Proteomics* **2005**, *4* (11), 1826–30.
- (14) Guo, T.; Rudnick, P. A.; Wang, W.; Lee, C. S.; Devoe, D. L.; Balgley, B. M. Characterization of the human salivary proteome by capillary isoelectric focusing/nanoreversed-phase liquid chromatography coupled with ESI-tandem MS. *J. Proteome Res.* **2006**, *5* (6), 1469–78.
- (15) Walz, A.; Stuhler, K.; Wattenberg, A.; Hawranke, E.; Meyer, H. E.; Schmalz, G.; Bluggel, M.; Ruhl, S. Proteome analysis of glandular parotid and submandibular-sublingual saliva in comparison to whole human saliva by two-dimensional gel electrophoresis. *Proteomics* **2006**, *6* (5), 1631–9.
- (16) Hardt, M.; Thomas, L. R.; Dixon, S. E.; Newport, G.; Agabian, N.; Prakobphol, A.; Hall, S. C.; Witkowska, H. E.; Fisher, S. J. Toward defining the human parotid gland salivary proteome and peptidome: identification and characterization using 2D SDS-PAGE, ultrafiltration, HPLC, and mass spectrometry. *Biochemistry* **2005**, *44* (8), 2885–99.
- (17) Denny, P.; Hagen, F. K.; Hardt, M.; Liao, L.; Yan, W.; Arellano, M.; Bassilian, S.; Bedi, G. S.; Boontheung, P.; Cociorva, D.; Delahunty, C. M.; Denny, T.; Dunsmore, J.; Faull, K. F.; Gilligan, J.; Gonzalez-Begne, M.; Halgand, F.; Hall, S. C.; Han, X.; Henson, B.; Hewel, J.; Hu, S.; Jeffrey, S.; Jiang, J.; Loo, J. A.; Ogorzalek Loo, R. R.; Malamud, D.; Melvin, J. E.; Miroshnychenko, O.; Navazesh, M.; Niles, R.; Park, S. K.; Prakobphol, A.; Ramachandran, P.; Richert, M.; Robinson, S.; Sondej, M.; Souda, P.; Sullivan, M. A.; Takashima, J.; Than, S.; Wang, J.; Whitelegge, J. P.; Witkowska, H. E.; Wolinsky, L.; Xie, Y.; Xu, T.; Yu, W.; Ytterberg, J.; Wong, D. T.; Yates, J. R., 3rd; Fisher, S. J. The proteomes of human parotid and submandibular/sublingual gland salivas collected as the ductal secretions. *J. Proteome Res.* **2008**, *7* (5), 1994–2006.
- (18) Ryu, O. H.; Atkinson, J. C.; Hoehn, G. T.; Illei, G. G.; Hart, T. C. Identification of parotid salivary biomarkers in Sjogren's syndrome by surface-enhanced laser desorption/ionization time-of-flight mass spectrometry and two-dimensional difference gel electrophoresis. *Rheumatology* **2006**, *45* (9), 1077–86.
- (19) Giusti, L.; Baldini, C.; Bazzichi, L.; Ciregia, F.; Tonazzini, I.; Mascia, G.; Giannaccini, G.; Bombardieri, S.; Lucacchini, A. Proteome analysis of whole saliva: a new tool for rheumatic diseases—the example of Sjogren's syndrome. *Proteomics* **2007**, *7* (10), 1634–43.
- (20) Hu, S.; Zhou, M.; Jiang, J.; Wang, J.; Elashoff, D.; Gorr, S.; Michie, S. A.; Spijkervet, F. K.; Bootsma, H.; Kallenberg, C. G.; Vissink, A.; Horvath, S.; Wong, D. T. Systems biology analysis of Sjogren's syndrome and mucosa-associated lymphoid tissue lymphoma in parotid glands. *Arthritis Rheum.* **2009**, *60* (1), 81–92.
- (21) Li, Y. B.; Wang, R.; Wu, H. L.; Li, Y. H.; Zhong, L. J.; Yu, H. M.; Li, X. J. Serum amyloid A mediates the inhibitory effect of Ganoderma lucidum polysaccharides on tumor cell adhesion to endothelial cells. *Oncol. Rep.* **2008**, *20* (3), 549–56.
- (22) Ding, Q. W.; Zhang, Y.; Wang, Y.; Wang, Y. N.; Zhang, L.; Ding, C.; Wu, L. L.; Yu, G. Y. Functional vanilloid receptor-1 in human submandibular glands. *J. Dent. Res.* **2010**, *89* (7), 711–6.
- (23) Zhang, Y.; Xiang, B.; Li, Y. M.; Wang, Y.; Wang, X.; Wang, Y. N.; Wu, L. L.; Yu, G. Y. Expression and characteristics of vanilloid

receptor 1 in the rabbit submandibular gland. *Biochem. Biophys. Res. Commun.* **2006**, *345* (1), 467–73.

(24) Ogawa, Y. Immunocytochemistry of myoepithelial cells in the salivary glands. *Prog. Histochem. Cytochem.* **2003**, *38* (4), 343–426.

(25) Baron, A.; Barrett-Vesponne, N.; Featherstone, J. Purification of large quantities of human salivary cystatins S, SA and SN: their interactions with the model cysteine protease papain in a non-inhibitory mode. *Oral Dis.* **1999**, *5* (4), 344–53.

(26) Messana, I.; Cabras, T.; Pisano, E.; Sanna, M. T.; Olianias, A.; Manconi, B.; Pellegrini, M.; Paludetti, G.; Scarano, E.; Fiorita, A.; Agostino, S.; Contucci, A. M.; Calo, L.; Picciotti, P. M.; Manni, A.; Bennick, A.; Vitali, A.; Fanali, C.; Inzitari, R.; Castagnola, M. Trafficking and postsecretory events responsible for the formation of secreted human salivary peptides: a proteomics approach. *Mol. Cell. Proteomics* **2008**, *7* (5), 911–26.

(27) Li, Y. M.; Zhang, Y.; Xiang, B.; Zhang, Y. Y.; Wu, L. L.; Yu, G. Y. Expression and functional analysis of beta-adrenoceptor subtypes in rabbit submandibular gland. *Life Sci.* **2006**, *79* (22), 2091–8.

(28) Cabras, T.; Castagnola, M.; Inzitari, R.; Ekstrom, J.; Isola, M.; Riva, A.; Messana, I. Carbachol-induced in vitro secretion of certain human submandibular proteins investigated by mass-spectrometry. *Arch. Oral Biol.* **2008**, *53* (11), 1077–83.

(29) Whitson, S. W.; Hand, A. R. Isoproterenol-induced changes in glutathione metabolism in the rat parotid gland. *Arch. Oral Biol.* **1984**, *29* (2), 137–40.

(30) Ahmed, N.; Ramjeesingh, M.; Wong, S.; Varga, A.; Garami, E.; Bear, C. E. Chloride channel activity of ClC-2 is modified by the actin cytoskeleton. *Biochem. J.* **2000**, *352* (Pt 3), 789–94.

(31) Busch, L.; Sterin-Borda, L.; Borda, E. Differences in the regulatory mechanism of amylase release by rat parotid and submandibular glands. *Arch. Oral Biol.* **2002**, *47* (10), 717–22.

(32) Kongo, H.; Hirono, C.; Sugita, M.; Iwasa, Y.; Shiba, Y. Involvement of cytoskeletal integrity in the regulation of Cl<sup>-</sup> and amylase secretion from rat parotid acinar cells. *Biomed. Res.* **2008**, *29* (3), 131–9.

(33) Honda, K.; Yamada, T.; Endo, R.; Ino, Y.; Gotoh, M.; Tsuda, H.; Yamada, Y.; Chiba, H.; Hirohashi, S. Actinin-4, a novel actin-bundling protein associated with cell motility and cancer invasion. *J. Cell Biol.* **1998**, *140* (6), 1383–93.

(34) Fletcher, D. A.; Mullins, R. D. Cell mechanics and the cytoskeleton. *Nature* **2010**, *463* (7280), 485–92.

(35) Pollard, T. D.; Cooper, J. A. Actin, a central player in cell shape and movement. *Science* **2009**, *326* (5957), 1208–12.

(36) Kurashima, K.; D'Souza, S.; Szaszi, K.; Ramjeesingh, R.; Orłowski, J.; Grinstein, S. The apical Na<sup>(+)</sup>/H<sup>(+)</sup> exchanger isoform NHE3 is regulated by the actin cytoskeleton. *J. Biol. Chem.* **1999**, *274* (42), 29843–9.

(37) Perrin, D.; Moller, K.; Hanke, K. Soling, H. D., cAMP and Ca<sup>(2+)</sup>-mediated secretion in parotid acinar cells is associated with reversible changes in the organization of the cytoskeleton. *J. Cell Biol.* **1992**, *116* (1), 127–34.

(38) Perez, P.; Aguilera, S.; Olea, N.; Allende, C.; Molina, C.; Brito, M.; Barrera, M. J.; Leyton, C.; Rowzee, A.; Gonzalez, M. J. Aberrant localization of ezrin correlates with salivary acini disorganization in Sjogren's Syndrome. *Rheumatology* **2010**, *49* (5), 915–23.

(39) Kanno, H.; Horikawa, Y.; Hodges, R. R.; Zoukhri, D.; Shatos, M. A.; Rios, J. D.; Dartt, D. A. Cholinergic agonists transactivate EGFR and stimulate MAPK to induce goblet cell secretion. *Am. J. Physiol. Cell Physiol.* **2003**, *284* (4), C988–98.

(40) Keely, S. J.; Uribe, J. M.; Barrett, K. E. Carbachol stimulates transactivation of epidermal growth factor receptor and mitogen-activated protein kinase in T84 cells. Implications for carbachol-stimulated chloride secretion. *J. Biol. Chem.* **1998**, *273* (42), 27111–7.

(41) Robey, R. B.; Ruiz, O. S.; Baniqued, J.; Mahmud, D.; Espiritu, D. J.; Bernardo, A. A.; Arruda, J. A. SFKs, Ras, and the classic MAPK pathway couple muscarinic receptor activation to increased Na-HCO<sub>3</sub> cotransport activity in renal epithelial cells. *Am. J. Physiol. Renal Physiol.* **2001**, *280* (5), F844–50.

(42) Sukezane, T.; Oneyama, C.; Kakumoto, K.; Shibusaki, K.; Hanafusa, H.; Akagi, T. Human diploid fibroblasts are resistant to

MEK/ERK-mediated disruption of the actin cytoskeleton and invasiveness stimulated by Ras. *Oncogene* **2005**, *24* (36), 5648–55.

(43) Shi, L.; Cong, X.; Zhang, Y.; Ding, C.; Ding, Q. W.; Fu, F. Y.; Wu, L. L.; Yu, G. Y. Carbachol improves secretion in the early phase after rabbit submandibular gland transplantation. *Oral Dis.* **2010**, *16* (4), 351–9.